

Supplementary Material for: “Comparison of the Marcus and Pekar partitions for non-equilibrium, polarizable-continuum reaction-field solvation models”

Zhi-Qiang You, Jan-Michael Mewes, Andreas Dreuw, and John M. Herbert*

We have recently developed a general discretization procedure that we call the “switching/Gaussian” (SWIG) procedure.^{1,2} This approach eliminates the discontinuities in the solute’s potential energy surface, which arises from using the straightforward point-charge (PC) discretization or tessellation (as in the widely-used GEPOL algorithm³⁻⁵). These may arise due to tessellation algorithms that fail to treat nuclear perturbations in a symmetric fashion, or else due to the appearance or disappearance of grid points as the solute geometry changes.

We have previously reported in Ref. 6 that the PC-discretization solvation energies for a data set consisting of amino acids exhibit large variation observed between two asymmetric forms of the \mathbf{X} matrix, namely, $\mathbf{X} = \mathbf{DAS}$ versus $\mathbf{X} = \mathbf{SAD}^\dagger$. Gaussian blurring greatly reduces the magnitude of these variations, and we find that the same is true for the non-equilibrium solvation corrections in the present work. In Fig. S1, we compared $\delta_N(\mathbf{Q})$ computed with PC and SWIG discretization schemes. For both IEF-PCM and SS(V)PE, $\delta_N(\mathbf{Q})$ oscillate as a function of grid density, but the PC values of $\delta_N(\mathbf{Q})$ are much larger than the SWIG values. The corresponding vertical excitation energies (the first-order ptSS energy and VIE) are shown in Figs. S2 and S3. Again the PC results are not smoothly converged and have oscillating features as the grid density increases. These observations are in agreement with the convergence tests for $\delta_N(\mathbf{Q})$.

Finally, we consider the eigenvalue spectrum of the matrix \mathbf{Q} , depending on how the matrix elements D_{ii} are defined [Eq. (45) versus Eq. (46)]. In particular, let us consider the example in Fig. 3(a): aqueous histidine at the AMBER99 level. When the cavity surface is discretized using $N = 590$ Lebedev points per atomic sphere, there is close agreement between IEF-PCM and SS(V)PE solvation energies, but for $N = 770$ the solvation energies differ by > 10 kcal/mol. The IEF-PCM results converge smoothly with respect to N , but for SS(V)PE the $N = 770$ point represents a significant anomaly in the otherwise smooth convergence with N . In Fig. S4 we

*To whom correspondence should be addressed

compare the spectrum of \mathbf{Q} , for $N = 590$ and $N = 770$, using three different models. The first is IEF-PCM when the locally-spherical approximation $D_{ii} = -S_{ii}/2R_I$ [Eq. (46)] is employed, and we regard this as something of a benchmark given the smooth convergence of IEF-PCM solvation energies with respect to N and the fact that Eq. (46) guarantees that \mathbf{Q} is negative-definite,² as it ought to be. The other two models are IEF-PCM and SS(V)PE using the sum rule of Eq. (45) to define D_{ii} .

For the most part, there is excellent agreement between the eigenvalue spectra for these three approaches, except for the largest eigenvalues. In the well-behaved $N = 590$ case [Fig. S4(a)], both IEF-PCM and SS(V)PE based on the sum rule exhibit some (but relatively few) positive eigenvalues, precisely 12 (of 3,118) in the former case and 26 in the latter, and the magnitudes of these positive eigenvalues are not much different from the rest of the spectrum. For the problematic $N = 770$ case, however, where IEF-PCM based on the sum rule behaves in a reasonable way but SS(V)PE exhibits an anomaly in the value of W_{pol} , the situation is quite different. For IEF-PCM based on the sum rule, the small number of positive eigenvalues (32 of 3,936) have magnitudes that are similar to the $N = 590$ discretization for the same model, and indeed the solvation energies are about the same as well. For SS(V)PE, 60 of 3,936 eigenvalues are positive but the largest of these are several orders of magnitude larger than most of the rest of the eigenvalue distribution [see Fig. S4(b)] and several orders of magnitude larger than the largest positive eigenvalues in the $N = 590$ case. In general we find that when the sum rule [Eq. (45)] is used, the SS(V)PE model (but not IEF-PCM) occasionally affords an out-of-line solvation energy, and in each case that we have seen, this is associated with anomalously large eigenvalues of \mathbf{Q} .

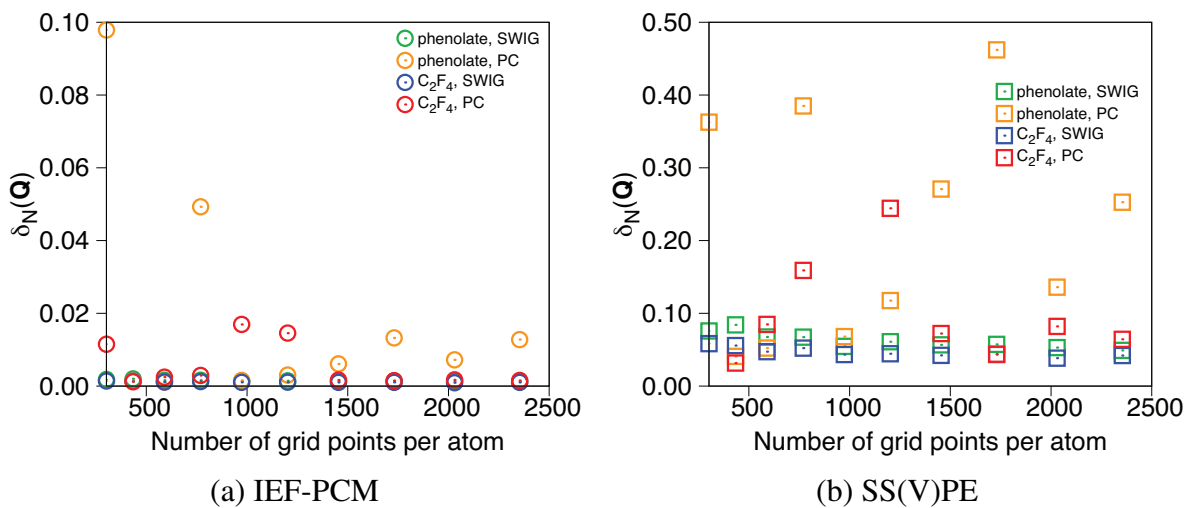


Figure S1: Convergence of the normalized norms of the matrix $\mathbf{Q} - \mathbf{Q}^\dagger$ computed with PC and SWIG discretization schemes, as a function of the number of Lebedev grid points per atomic sphere, for phenolate and for $C_2H_4 \cdots C_2F_4$.

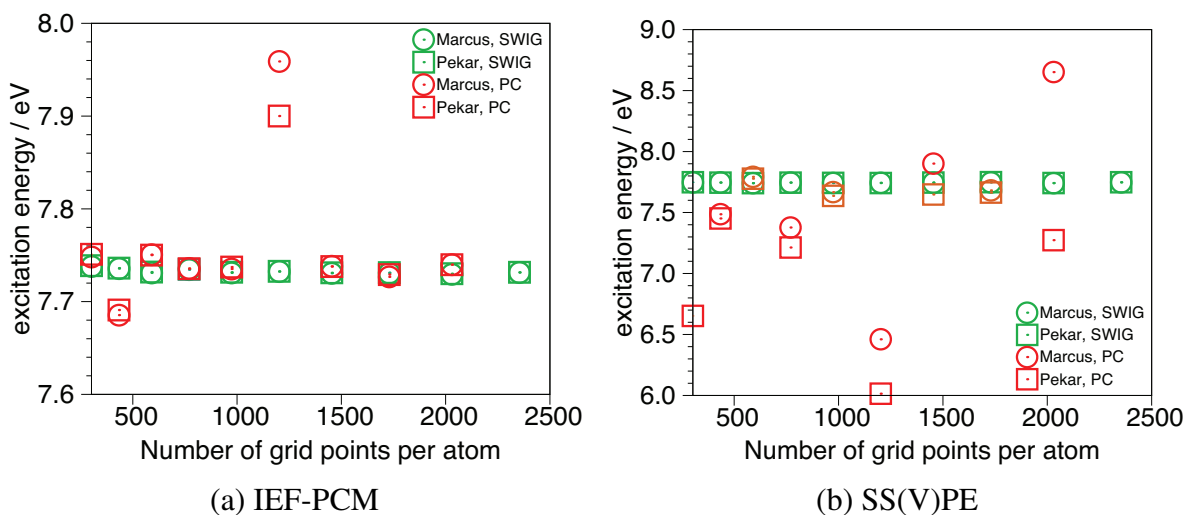


Figure S2: Convergence of the first-order ptSS excitation energy computed with PCM and SWIG discretization schemes as a function of the number of Lebedev grid points per atomic sphere, for $C_2H_4 \cdots C_2F_4$.

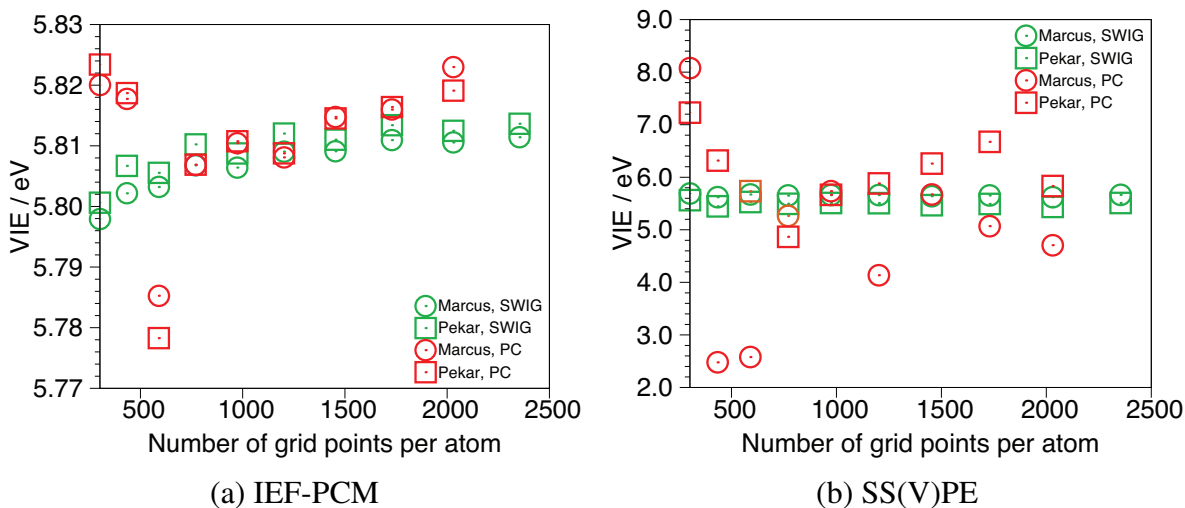


Figure S3: Convergence of the VIEs computed with PC and SWIG discretization schemes as a function of the number of Lebedev grid points per atomic sphere, for phenolate.

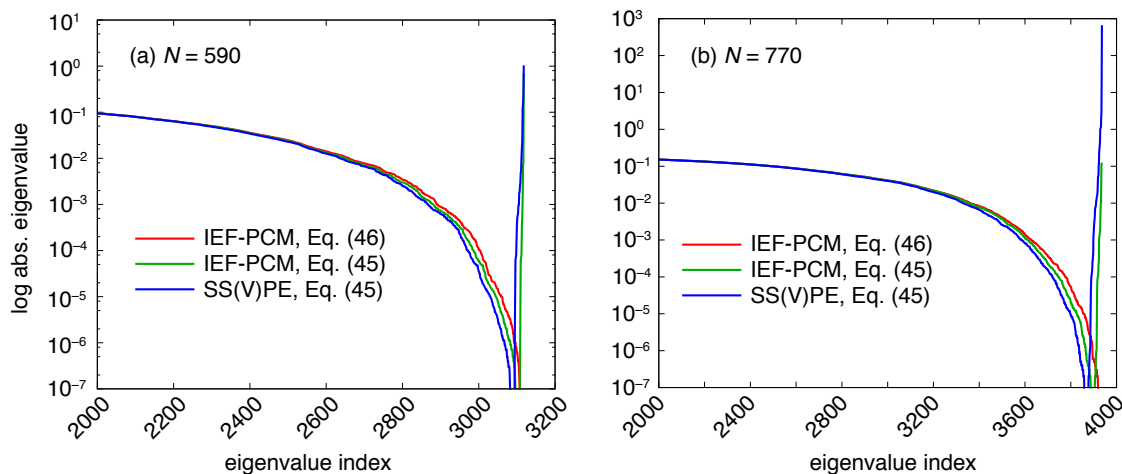


Figure S4: Distribution of eigenvalues of \mathbf{Q} for aqueous histidine at the AMBER99 level, using (a) 590 and (b) 770 Lebedev grid points per atomic sphere. The eigenvalues are arranged in increasing order and the first 2000 of them are not shown. The horizontal axis is simply a counter, and on the vertical axis we plot $\log(|x|)$ of the eigenvalues x (in atomic units), hence the sharp decrease to zero indicates where the eigenvalues go from negative to positive, and the rightmost parts of the distributions are the positive eigenvalues. Results are shown using the sum rule [Eq. (45)] to define D_{ii} and also the locally-spherical approximation that we prefer [Eq. (46)]. Note that both the horizontal and vertical scales are different in the two panels.

References

- (1) A. W. Lange, and J. M. Herbert *J. Chem. Phys.* **133**, 24411 (2010).
- (2) A. W. Lange, and J. M. Herbert *J. Phys. Chem. Lett.* **1**, 556 (2010).
- (3) J. L. Pascual-Ahuir, and E. Silla *J. Comput. Chem.* **11**, 1047 (1990).
- (4) E. Silla, and J. L. Pascual-Ahuir *J. Comput. Chem.* **12**, 1077 (1991).
- (5) J. L. Pascual-Ahuir, E. Silla, and I. Tuñon *J. Comput. Chem.* **15**, 1127 (1994).
- (6) A. W. Lange, and J. M. Herbert *Chem. Phys. Lett.* **509**, 77 (2011).